J. Fluid Mech. (1983), *vol.* 127, *pp.* 539–561
Printed in Great Britain

Shock dynamics in non-uniform media

By C. J. CATHERASOO AND B. STURTEVANT
Graduate Aeronautical Laboratories, California Institute of Technology, Pasadena, CA 91125

(Received 12 March 1982)

The theory of shock dynamics in two dimensions is reformulated to treat shock propagation in a non-uniform medium. The analysis yields a system of hyperbolic equations with source terms representing the generation of disturbances on the shock wave as it propagates into the fluid non-uniformities. The theory is applied to problems involving the refraction of a plane shock wave at a free plane gaseous interface. The 'slow–fast' interface is investigated in detail, while the 'fast–slow' interface is treated only briefly. Intrinsic to the theory is a relationship analogous to Snell's law of refraction at an interface. The theory predicts both regular and irregular (Mach) refraction, and a criterion is developed for the transition from one to the other. Quantitative results for several different shock strengths, angles of incidence and sound-speed ratios are presented. An analogy between shock refraction and the motion of a force field in unsteady one-dimensional gasdynamics is pointed out. Also discussed is the limiting case for a shock front to be continuous at the interface. Comparison of results is made with existing experimental data, with transition calculations based on three-shock theory, and with the simple case of normal interaction.

1. Introduction

When a plane shock wave propagates through a non-uniform medium, the wavefront becomes curved and distorted, as in the diffraction and refraction of shock waves in turbulence and in substances of varying sound speed. Similar distortions of shock fronts occur even in uniform media when the fronts pass over curved boundaries, as in shock diffraction over a wedge. The latter problem has received considerable attention in the past, and it is now possible to treat diffraction over bodies with exact numerical calculation (Shankar, Kutler & Anderson 1978; Kutler & Shankar 1977), or with an approximate theory, known as shock dynamics, due to Whitham (1957, 1959). This approximate theory has been extended by Collins & Chen (1970, 1971), to cover shock propagation in a non-uniform medium. However, their work has not received much attention, despite the fact that there does not exist a method for calculating such flows that properly preserves the sharpness of discontinuities, other than the method of characteristics for fully 2- or 3-dimensional non-steady flow.

Shock dynamics is the nonlinear analogue of geometrical acoustics. It accounts for the fact that in non-uniform propagation the rays (normals to the shock front) are not straight and parallel. It treats the distortion of wavefronts in terms of disturbances which propagate transversely along the fronts. As with geometrical acoustics, the theory does *not* treat the field behind the wave fronts and therefore is not applicable to problems in which disturbances generated by processes *behind* the shock overtake and modify it. It differs from geometrical acoustics in that the disturbances may either steepen or spread out by nonlinearity, a property unique to finite-amplitude waves.

In this paper, Whitham's theory of shock dynamics is generalized to treat the effects on shock propagation of fluid non-uniformities in the undisturbed medium ahead of the shock front. The governing equations are applied to simple problems involving the refraction of a plane shock wave at a free plane gaseous interface, and the results are compared with existing experimental data.

2. The governing equations

2.1. *Derivation of the characteristic equations*

The derivation of the equations that account for the generation and propagation of disturbances on the shock front follows the analysis of Whitham (1957). First, a relation between the shock Mach number M, the ray-tube area A and variation in fluid properties is obtained as in CCW theory (Chester 1954; Chisnell 1955, 1957; Whitham 1958) for shock propagation in a channel of slowly varying area, and, in this case, with slowly varying sound speed a_0 ahead of the shock. Since shock dynamics is formulated to treat only perfect gases, the changes in a_0 may be caused by spatial variations in the thermodynamic state of the fluid, or by spatial variations in the concentration of mixtures of perfect gases, or both. Hence, in the formulation of the theory it is necessary to consider imposed variations of temperature T_0 and specific heat ratio γ, together with related variations in density ρ_0, and of pressure p_0, which would result if body forces were present. It is convenient to express these variations in terms of γ, a_0 and p_0. The resulting equation, which treats *any* spatial variations in the perfect gas ahead of the shock front, is

$$\frac{M\lambda}{M^2-1}dM+\frac{dA}{A}+f\,d\gamma+g\frac{da_0}{a_0}+h\frac{dp_0}{p_0}=0, \tag{2.1}$$

where

$$\lambda(M,\gamma)=\left(1+\frac{2}{\gamma+1}\frac{1-\mu^2}{\mu}\right)\left(1+2\mu+\frac{1}{M^2}\right), \tag{2.2}$$

$$f(M,\gamma)=\frac{g(M,\gamma)}{\gamma(\gamma+1)}(\mu-\gamma), \tag{2.3}$$

$$g(M,\gamma)=1+\frac{2\mu(M^2-1)}{(\gamma-1)M^2+2}, \tag{2.4}$$

$$h(M,\gamma)=\frac{1}{2\gamma(M^2-1)}\left[2(M^2-1)+\mu\{2\gamma M^2-(\gamma-1)\}-\frac{(\gamma+1)^2\mu M^2}{(\gamma-1)M^2+2}\right], \tag{2.5}$$

$$\mu(M,\gamma)=\left[\frac{(\gamma-1)M^2+2}{2\gamma M^2-(\gamma-1)}\right]^{\frac{1}{2}}. \tag{2.6}$$

In general, (2.1) agrees with the expression derived by Collins & Chen (1971), except for the coefficients of $d\gamma$ and dp_0.

Next, an orthogonal system of coordinates (α, β) is introduced, where α = constant are the shock fronts and β = constant are the rays. Relations between shock velocity U and ray inclination θ are derived from differential geometry (Whitham 1957):

$$\frac{\partial\theta}{\partial\alpha}=-\frac{1}{A}\frac{\partial U}{\partial\beta}, \tag{2.7}$$

$$\frac{\partial\theta}{\partial\beta}=\frac{1}{U}\frac{\partial A}{\partial\alpha}, \tag{2.8}$$

where $U=a_0 M$, and a_0, M and U are functions of α and β.

The above equations are combined and put in characteristic form to yield the governing equations in the shock-based coordinate system:

$$d\theta \pm d\omega = -(F \pm cG)\, d\alpha \quad \text{on} \quad \frac{d\beta}{d\alpha} = \pm c, \tag{2.9}$$

where

$$F = \frac{M}{A}\frac{\partial a_0}{\partial \beta}, \tag{2.10}$$

$$G = \frac{A}{a_0 M}\left[f\frac{\partial \gamma}{\partial \alpha} + \frac{g}{a_0}\frac{\partial a_0}{\partial \alpha} + \frac{h}{p_0}\frac{\partial p_0}{\partial \alpha}\right], \tag{2.11}$$

$$c = \frac{a_0}{A}\left(\frac{M^2-1}{\lambda}\right)^{\frac{1}{2}}, \tag{2.12}$$

$$\omega = \int_1^M \left[\frac{\lambda(m,\gamma)}{m^2-1}\right]^{\frac{1}{2}} dm. \tag{2.13}$$

Finally, the system is transformed back to the physical plane. The resulting equations are

$$d\theta \pm d\omega = -\frac{1}{\tan\theta \pm \nu}\left[\frac{1}{a_0}\left\{(-\tan\theta \pm \nu g)\frac{\partial a_0}{\partial x} + (1 \pm \nu g \tan\theta)\frac{\partial a_0}{\partial y}\right\}\right.$$
$$\left. \pm \nu f\left(\frac{\partial \gamma}{\partial x} + \tan\theta\frac{\partial \gamma}{\partial y}\right) \pm \frac{\nu h}{p_0}\left(\frac{\partial p_0}{\partial x} + \tan\theta\frac{\partial p_0}{\partial y}\right)\right] dy \tag{2.14}$$

on the characteristics

$$\frac{dy}{dx} = \frac{\tan\theta \pm \nu}{1 \mp \nu\tan\theta}, \tag{2.15}$$

where

$$\nu = \frac{1}{M}\left(\frac{M^2-1}{\lambda}\right)^{\frac{1}{2}}. \tag{2.16}$$

The governing equations (2.14) form a hyperbolic system which describes wavelike disturbances that travel in opposite directions along the shock front, and carry information about changes of M and θ. The characteristics are real, and their slope dy/dx is an increasing function of M, so that a disturbance carrying an increase in shock strength steepens, whereas a disturbance carrying a decrease in shock strength spreads out. When an expansive disturbance on the shock front results in a simple wave (expansion fan), we refer to it as a *shock–expansion*. On the other hand, a compressive disturbance eventually breaks and forms a discontinuity of M and θ on the shock front, the jump conditions across which have been given by Whitham (1957). The locus of this discontinuity is called a *shock–shock*. Physically, the shock–shock is the locus of the triple-shock intersection, and its occurrence signals the formation of a Mach stem.

The governing equations (2.14) are similar to those obtained by Whitham (1957) for the case of a uniform medium (γ, a_0, p_0 = constant), but, in general, they differ through the appearance of 'source' terms on the right-hand side. The source terms contain the *gradients* of the independent variables γ, a_0 and p_0. Indeed, for the uniform medium case, the gradients are zero and the source terms vanish, so that we recover the equations given by Whitham. Thus, in this formulation, disturbances may be generated on the shock front by boundary conditions such as wall curvature, as well as by non-uniformities in the medium ahead of the shock. We note that the source terms are implicit, since they contain the dependent variables M and θ, as well as the independent variables γ, a_0 and p_0.

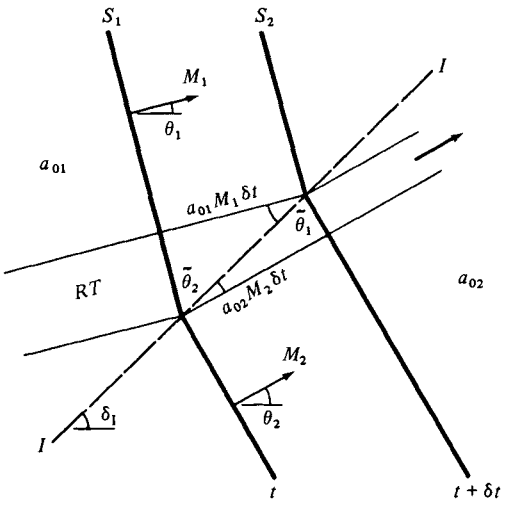

FIGURE 1. The contact surface discontinuity: S_1, S_2, shock–front positions at two successive times t and $t+\delta t$; I, interface; RT, ray tube.

2.2. *The contact discontinuity*

For shock dynamics in a non-uniform medium, one must account for the possible occurrence of discontinuities in fluid properties, that is, *contact discontinuities*, ahead of the shock front. We consider an element of interface inclined at an angle δ_I to the x-axis, as shown in figure 1. To remove the x-dependence from the source terms, we introduce a simple rotation of the shock and the interface through an angle $-\delta_I$, so that the interface lies parallel to the x-axis. Then a_0, γ and p_0 become functions of y only, and (2.14) reduce to

$$d\tilde{\theta} \pm d\omega = -\frac{1}{\tan\tilde{\theta} \pm \nu}\left[(1 \pm \nu g \tan\tilde{\theta})\frac{da_0}{a_0} \pm \nu \tan\tilde{\theta}\left(f\,d\gamma + h\frac{dp_0}{p_0}\right)\right] \tag{2.17}$$

on the characteristics

$$\frac{dy}{dx} = \frac{\tan\tilde{\theta} \pm \nu}{1 \mp \nu \tan\tilde{\theta}},$$

where $\tilde{\theta}$, the angle between the rays of the local shock front and the interface, is given by

$$\tilde{\theta} = \theta - \delta_I. \tag{2.18}$$

If we apply (2.17) to a pair of characteristics that intersect a contact interface across which there are *infinitesimal* changes of sound speed da_0, specific heat ratio $d\gamma$ and pressure dp_0, on eliminating the terms in a_0 we obtain the simple result

$$\tan\tilde{\theta}\,d\tilde{\theta} = -\frac{dU}{U}. \tag{2.19}$$

Then, assuming that the effects of an interface carrying *finite* changes can be built up by summing the infinitesimal changes, (2.19) is integrated to yield

$$\frac{U}{\cos\tilde{\theta}} = \text{constant}. \tag{2.20}$$

Hence (2.17) provide *exactly* the condition required for a continuous shock front across such an interface, a condition that is analogous to Snell's law of refraction.

By eliminating the terms in $d\tilde{\theta}$ from (2.17), we obtain

$$(\tan^2\tilde{\theta}-\nu^2)\frac{dM}{M}=\nu^2\left[(1-g\tan^2\tilde{\theta})\frac{da_0}{a_0}-\tan^2\tilde{\theta}\left(f\,d\gamma+h\frac{dp_0}{p_0}\right)\right]. \tag{2.21}$$

In order to demonstrate the properties of the equations in the simplest way possible, we consider in the remainder of this work the case $\gamma, p_0 =$ constant, that is, the medium is a perfect gas in which only variations of temperature occur. Then the last two terms in (2.21) vanish and the equation reduces to an ordinary differential equation in M and a_0:

$$\frac{dM}{da_0}=\frac{\nu^2M(U^2-gV^2)}{a_0(V^2-\nu^2U^2)}, \tag{2.22}$$

where

$$U=a_0M, \tag{2.23}$$

$$V=\left[\left(\frac{a_{01}M_1}{\cos\tilde{\theta}_1}\right)^2-(a_0M)^2\right]^{\frac{1}{2}}. \tag{2.24}$$

Given the shock strength and sound speed on one side of the interface, say M_1 and a_{01}, the ordinary differential equation (2.22) can be solved to yield the shock strength M_2 on the other side, where the sound speed is a_{02}. To complete the solution of the jump conditions across the interface, the slope of the shock front in the secondary region is found from (2.20). Then the final step is to restore the shock and the interface to their original positions by another simple rotation through an angle $+\delta_{\mathrm{I}}$.

It is interesting to consider the direction of crossing of the ray tubes at the interface. Figure 1 has been drawn to illustrate the results of shock refraction for the case of $\theta<\delta_{\mathrm{I}}$, and shown in the figure is a ray tube consisting of a bundle of rays. For the case of $\theta<\delta_{\mathrm{I}}$, the ray tubes cross the interface from region 1 to region 2, while, for the case of $\theta>\delta_{\mathrm{I}}$, the ray tubes cross the interface in the opposite direction. Since the ray tubes represent the channelling of energy between rays, the direction in which the ray tubes cross the interface indicates the region into which the refracted shock is growing. When $\theta=\delta_{\mathrm{I}}$, the shock is normal to the interface, and the ray tubes do not cross the interface. This condition is identical to that which is applied at a solid boundary in the analysis of shock diffraction using the theory of shock dynamics in a *uniform* medium.

3. Shock refraction

As a demonstration of the application of the theory, we consider problems involving a plane shock wave incident at some angle on a free plane gaseous interface across which there exists a finite difference in sound speed (Jahn 1956; Abd-el-Fattah, Henderson & Lozzi 1976). Two different problems are discussed. In the first problem, only a gaseous interface is present, while the second involves a solid boundary as well. The problems are designed to be self-similar, and they have been chosen for consideration because non-simple regions do not appear in the flow field. For regular refraction the effects of the interface are only local so, in fact, regular refraction can be solved exactly by three-shock theory. However, shock dynamics also predicts irregular refraction, so even these simple cases are interesting.

As the first example (problem 1) we choose the simplest configuration that contains all the important effects; namely one in which the contact interface is wedge-shaped, with one of the sides aligned parallel with the undisturbed shock front and the other lying at an angle δ_{I} with the x-axis, as shown in figure 2. S_1 is the incident shock front and S_2 is the shock front at a subsequent time after interaction with the interface.

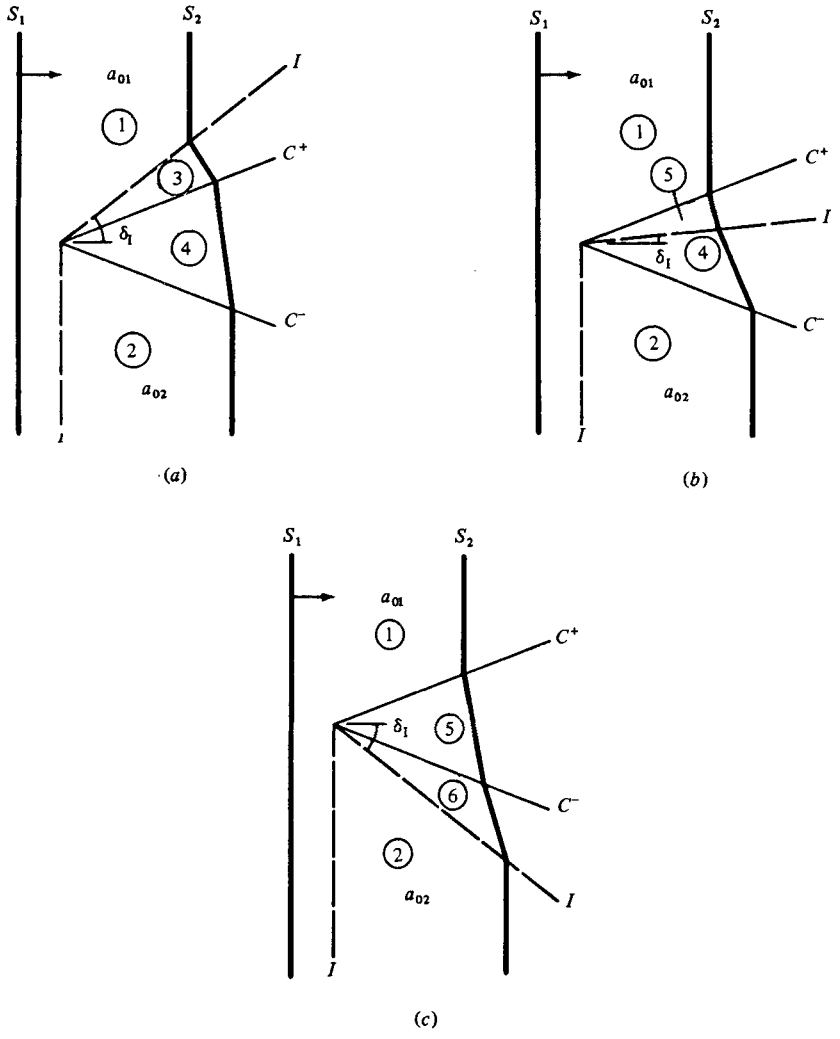

FIGURE 2. Configurations for problem 1: (*a*) contact surface above leading C^+ characteristic; (*b*) contact surface between leading C^+ and C^- characteristics; (*c*) contact surface below leading C^- characteristic; S_1, incident shock front; S_2, shock front after interaction with interface; I, interface.

The shock transmits through the vertical portion of the contact surface and refracts from the other. Regions 1–6 in figure 2 are uniform regions. The shock in region 2 provides the lower boundary condition in this problem, and is calculated exactly from the equations of one-dimensional gasdynamics, while in regions 3–6 the shock conditions are calculated from the approximate theory developed here.

In the second example (problem 2) a solid wall is introduced below the sloping interface, at an angle δ_W with the x-axis, as shown in figure 3, and the boundary condition imposed here is that the shock is always normal to the wall. Regions 1–4 are uniform and they are calculated from shock dynamics theory.

As shown in figures 2 and 3, different cases are possible for each problem, depending on the position of the interface with respect to the leading C^+ and C^- characteristics. In problem 1 the interface may lie above the leading C^+ characteristic, it may lie

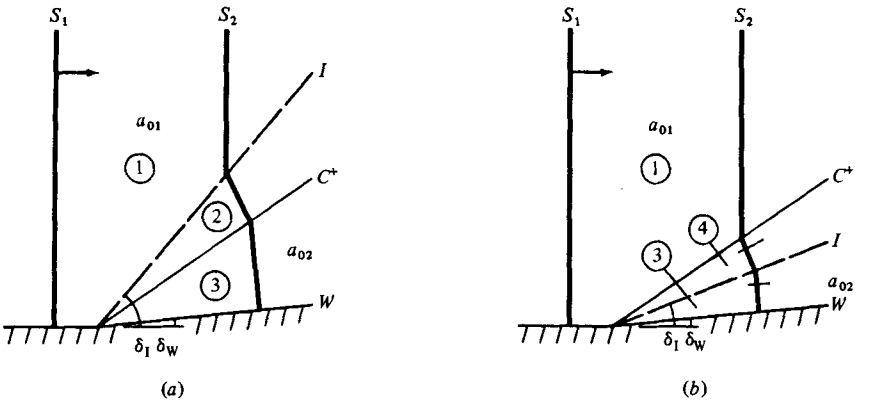

FIGURE 3. Configurations for problem 2: (*a*) contact surface above leading C^+ characteristic; (*b*) contact surface between leading C^+ characteristic and wall; S_1, incident shock front; S_2, shock front after interaction with interface; I, interface; W, wall.

between the leading C^+ and C^- characteristics, or it may lie below the leading C^- characteristic. Likewise, in problem 2 the interface may lie above the leading C^+ characteristic, or it may lie between the leading C^+ characteristic and the wall. When the interface lies above the leading C^+ characteristic or below the leading C^- characteristic, the steepness of the interface prevents disturbances on the shock front from propagating outward from the interface, and these are cases of *regular* refraction. However, in problem 1, when the interface lies between the leading C^+ and the leading C^- characteristics, or in problem 2, when it lies between the leading C^+ characteristic and the wall, the disturbances propagate outward from the interface, resulting in *irregular* refraction. Thus shock dynamics theory for a non-uniform medium models both regular and irregular refraction. This is not the case for shock dynamics in a uniform medium, where, for the reflection of a shock by a solid wedge, the theory predicts a very tiny Mach stem for conditions under which regular reflection actually occurs (Whitham 1957).

In order to demonstrate the quantitative behaviour of the theory, shock refraction has been calculated for several different values of δ_I, δ_W, a_0 and M, including values taken from the experiments performed by Jahn (1956), and from the experimental and theoretical work of Henderson's group (Abd-el-Fattah *et al.* 1976; Abd-el-Fattah & Henderson 1978). The case $a_{02} > a_{01}$ (the 'slow–fast' interaction) has been investigated in detail for both problems, while the case $a_{02} < a_{01}$ (the 'fast–slow' interaction) has so far been treated only for problem 1. Typical results are presented in tables 1–4.

The problems are solved using the interface jump conditions (2.20) and (2.22), the shock–shock jump conditions, and the invariance of $\theta \pm \omega$ in the uniform regions and in the simple waves. For the regular-refraction cases the conditions behind the interface are determined directly from the known conditions ahead of the interface, and the remaining region is then determined from the boundary conditions. However, for the irregular refraction cases, since none of the conditions in the two regions adjacent to the interface is known *a priori*, it is necessary to make a guess of one quantity, say the Mach number M, ahead of the interface and then to solve the equations iteratively. Unless otherwise stated, the computational accuracy for M in these cases is better than 0·001 %.

Although the theory of shock dynamics in a non-uniform medium is approximate

and provides information only about the main shock front, it has an important advantage over existing methods for calculating shock refraction at a gaseous interface, in that it is simple to apply and yields a unique solution. On the other hand, local solution of the full gasdynamics equations from three-shock theory (e.g. Taub 1947; Polachek & Seeger 1951; Henderson 1966) yields information about the reflected wave as well, but, in general, there are twelve possible roots, so that it is necessary to develop a criterion to determine which solution agrees best with experiment. This has been the source of considerable controversy.

3.1. *Problem* 1

A series of solutions for problem 1 with $M_1 = 5{\cdot}0$ and $a_{02}/a_{01} = 2{\cdot}0$ is given in table 1, and some typical cases are illustrated in figure 4. The uniform regions (1–6) are adjacent to simple waves (shock–expansions), or to discontinuities (shock–shocks or the contact surface). The shock front is continuous throughout, but the slope is discontinuous at the shock–shock and at the contact surface. Both the shock strength and slope vary continuously through the shock–expansions. As might be expected, for the slow–fast interaction the theory shows the shock to be concave-forward in the upper part of the flow field and convex-forward in the lower part.

For large interface angles, a regular-refraction solution is obtained, which contains two shock–expansions of opposite families, as shown in figure 4(*a*) (case 2). Shock dynamics theory predicts transition from regular to irregular refraction when the slope of the interface is equal to the slope of the characteristics in the region just behind the interface. This occurs when the uppermost characteristic of the shock–expansion between regions 3 and 4, designated here as C_t^+, approaches the contact surface, and region 3 vanishes. Then,

$$\delta_{I_t^+} = \arctan\left(\frac{dy}{dx}\right)\Big|_{C_t^+}, \tag{3.1}$$

where $\delta_{I_t^+}$ is the interface angle at transition, and dy/dx is given by (2.15), evaluated on C_t^+ (case 3). The criterion for transition from regular to irregular refraction, which arises naturally in this theory in terms of the slopes of the characteristics, is very similar to the 'sonic' condition proposed by Hornung, Oertel & Sandeman (1979) for shock diffraction over a wedge. We note that, at transition, the flow deflection angle is greatest, and designate this angle θ_{3t}.

Up to this point, the C^+ characteristics crossing the interface originate in region 1, and the direction of crossing is from above to below. However, a further decrease in δ_1 results in a reversal in the direction of crossing of the C^+ characteristics, which now originate from the corner. The C^+ characteristics emerging from the interface are steeper than those in region 1, and this results in the formation of a shock–shock discontinuity, which initially lies just above the interface (case 4), at an angle χ_1 with the x-axis. As the interface angle is decreased further, the shock–shock separates from the interface, as shown in figure 4(*b*) (case 5), and the upper shock–expansion becomes smaller, until it finally vanishes (case 6).

In cases 4–6, and in other cases to be encountered later, a characteristic lies just behind and adjacent to the interface. Under these conditions, a singularity develops in the expression (2.22) for dM/da_0, as a_0 approaches a_{02}. It can be shown that the singularity is a square-root singularity, so that dM/da_0 is integrable, and solutions exist for this range of interface angles.

Transition from regular to irregular refraction in shock dynamics theory is analogous to that which occurs in unsteady one-dimensional gasdynamics under the

$M_1 = 5{\cdot}0$, $\theta_1 = 0°$ and $a_{02}/a_{01} = 2{\cdot}0$
($M_2 = 3{\cdot}43$ and $\theta_2 = 0°$)

Case	δ_1	M_3	θ_3	M_4	θ_4	M_5	θ_5	M_6	θ_6	χ_1	χ_2
1	90·0°	3·56	0°	3·49	−2·3°	—	—	—	—	—	—
2	60·0°	3·73	18·3°	3·34	3·6°	—	—	—	—	—	—
3	55·7°	(4·07)	(32·2°)	3·31	4·9°	—	—	—	—	—	—
4	55·0°	—	—	3·29	5·7°	(8·71)	(52·3°)	—	—	55·0°	—
5	45·0°	—	—	3·16	11·1°	7·44	42·5°	—	—	48·0°	—
6	36·8°	—	—	3·10	13·6°	6·74	34·4°	—	—	42·8°	—
7	30·0°	—	—	3·06	15·4°	6·31	28·2°	—	—	38·9°	—
8	20·5°	—	—	2·94	20·5°	5·89	20·5°	—	—	34·6°	—
9	15·0°	—	—	2·78	28·1°	5·70	16·6°	—	—	32·4°	—
10	13·8°	—	—	(2·61)	(36·6°)	5·67	15·9°	—	—	32·0°	—
11	14·0°	—	—	—	—	5·66	15·7°	(3·01)	(71·9°)	31·9°	14·0°
12	0°	—	—	—	—	5·40	10·0°	3·39	57·3°	28·8°	6·1°
13	−23·3°	—	—	—	—	5·21	5·2°	4·13	33·1°	26·4°	−5·6°
14	−45·0°	—	—	—	—	5·12	3·0°	4·60	16·7°	25·3°	−14·1°
15	−71·0°	—	—	—	—	5·00	0°	4·78	5·9°	23·7°	−20·8°

Values in parentheses denote vanishingly small regions.

TABLE 1. Summary of calculated refraction parameters for problem 1

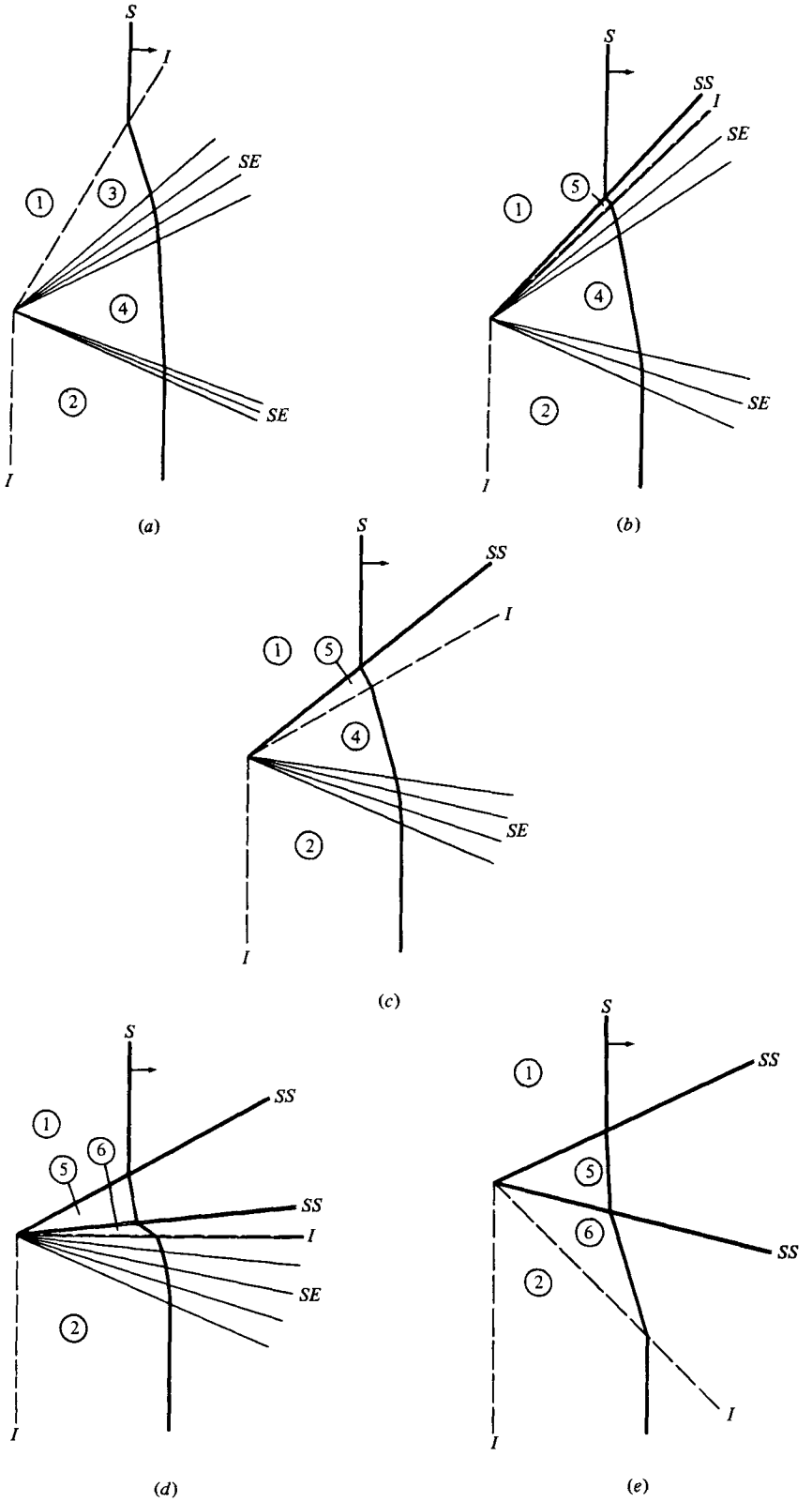

FIGURE 4. For caption see facing page.

action of a moving force field or 'leaky piston'. The force, which is a 'source' in gasdynamics, is analogous to the contact interface, which is a 'source' in shock dynamics. As shown by Hoffman (1967), a transition occurs from a shock-free solution, when the force is weak and supersonic, to a solution containing a shock, when the force is subsonic. In our case, a steeply inclined interface corresponds to a supersonic force, while a gradually sloping interface corresponds to a subsonic force. Hoffman showed that in an intermediate case, analogous to our cases 4–6, a characteristic in the (x, t)-plane lies adjacent to the force and behind it, while the characteristics ahead, between the force and the shock, lie at a finite angle to the force. For this case, a square-root singularity exists at the back of the force. The appearance of a characteristic adjacent to and at the back of a surface of discontinuity signifies a sonic condition well known in gasdynamics, a familiar example of which is the Chapman–Jouget detonation. The physical processes leading to this case are most easily understood for a force field (or contact region) or finite width (Hoffman 1967). Our use of the differential relation (2.22) is equivalent to treating the contact discontinuity as a region of finite width.

These results show that, if the interface is steep enough, the only mechanism by which concave curvature ('compressive' bending) can be induced on the shock is that provided by Snell's law, at or within the interface. However, for smaller interface angles, when the refraction is irregular, convex curvature ('expansive' bending) occurs at the interface, presumably because too much compressive bending occurs at the shock–shock. For very small interface angles, the shock–shock may be sufficiently weak that the interface once again becomes compressive, as shown below in case 9. The interpretation of shock refraction in these terms yields some additional insight to the rather startling solutions in one-dimensional gasdynamics put forward by Hoffman.

It is also interesting to note that there exists a finite range of interface angles (0·7° in this instance, between cases 3 and 4) in which no solution could be obtained for the irregular refraction case. It appears that this difficulty is associated with the formation of the shock–shock *on* the interface, and a similar difficulty occurs whenever a shock–shock lies on or immediately adjacent to the interface.

Shown in figure 4 (*c*) is the geometry of a simple irregular refraction, after the upper shock–expansion has vanished (case 7). As the interface angle continues to decrease, the shock front becomes normal to the interface (case 8) and then reverses curvature (case 9) from convex-forward at the interface to concave-forward. For case 8, in which we designate the interface angle as $\delta_{\mathrm{I_n}}$, we note that the shock fronts on both sides of the interface are normal to the interface, so that the ray tubes do not cross the interface. In other words, there is no transfer of energy across the interface, as discussed in §2.2. This case is identical with the diffraction of a shock by a solid wedge of angle $\delta_{\mathrm{I_n}}$.

For a further decrease in the slope of the interface, a second transition angle $\delta_{\mathrm{I_t^-}}$ is reached when the uppermost characteristic of the lower shock–expansion C_{t}^- approaches the contact surface, and region 4 vanishes, that is,

$$\delta_{\mathrm{I_t^-}} = \arctan\left(\frac{dy}{dx}\right)\Big|_{C_1^-}, \tag{3.2}$$

FIGURE 4. Solutions for problem 1 with $M_1 = 5{\cdot}0$ and $a_{02}/a_{01} = 2{\cdot}0$: (*a*) regular refraction, $\delta_{\mathrm{I}} = 60{\cdot}0°$ (case 2); (*b*) irregular refraction, $\delta_{\mathrm{I}} = 45{\cdot}0°$ (case 5); (*c*) irregular refraction, $\delta_{\mathrm{I}} = 30{\cdot}0°$ (case 7); (*d*) irregular refraction, $\delta_{\mathrm{I}} = 0°$ (case 12); (*e*) regular refraction, $\delta_{\mathrm{I}} = -45{\cdot}0°$ (case 14); *S*, shock front; *I*, interface; *SE*, shock–expansion; *SS*, shock–shock.

where dy/dx is evaluated on C_t^- (case 10). For $\delta_I < \delta_{I_t^-}$, the behaviour of the C^- characteristics is similar to the behaviour of the C^+ characteristics for $\delta_I < \delta_{I_t^+}$. The C^- characteristics that cross the interface now originate from the corner, instead of originating in region 1 as before, and the direction of crossing is now from below to above. The steepness of the C^- characteristics emerging from the interface results in the formation of a *second* shock–shock, which initially lies just above the interface (case 11), at an angle χ_2 with the x-axis. As shown in figure 4(*d*) (case 12), the shock–shock separates from the interface as the interface angle is decreased, and the lower shock–expansion becomes smaller, until it finally vanishes (case 13).

At this point (case 13), the interface lies on the leading C^- characteristic. When the interface lies below this characteristic, no information about the corner can propagate outward along the shock from the interface, so that the shock refraction at the interface becomes locally regular. A typical example is shown in figure 4(*e*) (case 14), in which we see that two shock–shocks of opposite families are present, but no shock–expansions.

This behaviour continues as the interface moves down toward the vertical. Both shock–shocks weaken, and as expected the shock front straightens out and its strength tends to the undisturbed value of M_1. However, in region 6, where the shock front has passed through two interfaces, the recovery is incomplete, and this may be attributed to reflection losses at each of the two interactions.

The solutions for this problem that involve two shock–expansions or two shock–shocks of opposite families are unusual, especially the latter, in which both the shock–shocks share a common Mach stem. Such solutions are the result of the unique properties of the characteristics in shock dynamics. It will be interesting to compare these predicted solutions with actual experimental results, when such results become available.

Before leaving this problem, we note that, although we have been considering the slow–fast interface, the preceding results embody the *form* of the solutions for the fast–slow interface as well. For the fast–slow interface we have $a_{02} < a_{01}$, $M_2 > M_1$ and $U_2 < U_1$, so that by interchanging region 1 with region 2 we get $a_{02} > a_{01}$, $M_2 < M_1$ and $U_2 > U_1$, which are exactly the boundary conditions for the slow–fast interface. Of course to get the *detailed* results for the fast–slow case, it is necessary to determine M_2 at the vertical part of the interface, and then to solve for the various regions as before.

3.2. *Problem 2*

Given in table 2 and shown in figures 5 and 6 are some typical results for problem 2. For any given incident shock strength and sound-speed ratio, two different sequences of solutions are obtained, depending on the wall angle δ_W. We note from the transition condition in problem 1 (case 3) that, when the interface angle is $\delta_{I_t^+}$, the flow deflection for regular refraction is maximum (θ_{3_t}), and that, in order to obtain a larger deflection, the flow adjusts itself by becoming irregular. Hence, for problem 2, in which a wall is present below the interface, if $\delta_W > \theta_{3_t}$, for δ_I decreasing from 90°, it might be expected that the solution will become irregular before δ_I reaches $\delta_{I_t^+}$. Indeed, for $\delta_W < \theta_{3_t}$, transition from regular to irregular refraction occurs at $\delta_I = \delta_{I_t^+}$, whereas for $\delta_W > \theta_{3_t}$, it occurs earlier and, as a consequence, there are two sequences to be considered. An interesting third sequence is obtained by keeping the interface and wall angles fixed, and observing the effects of reducing the incident shock strength.

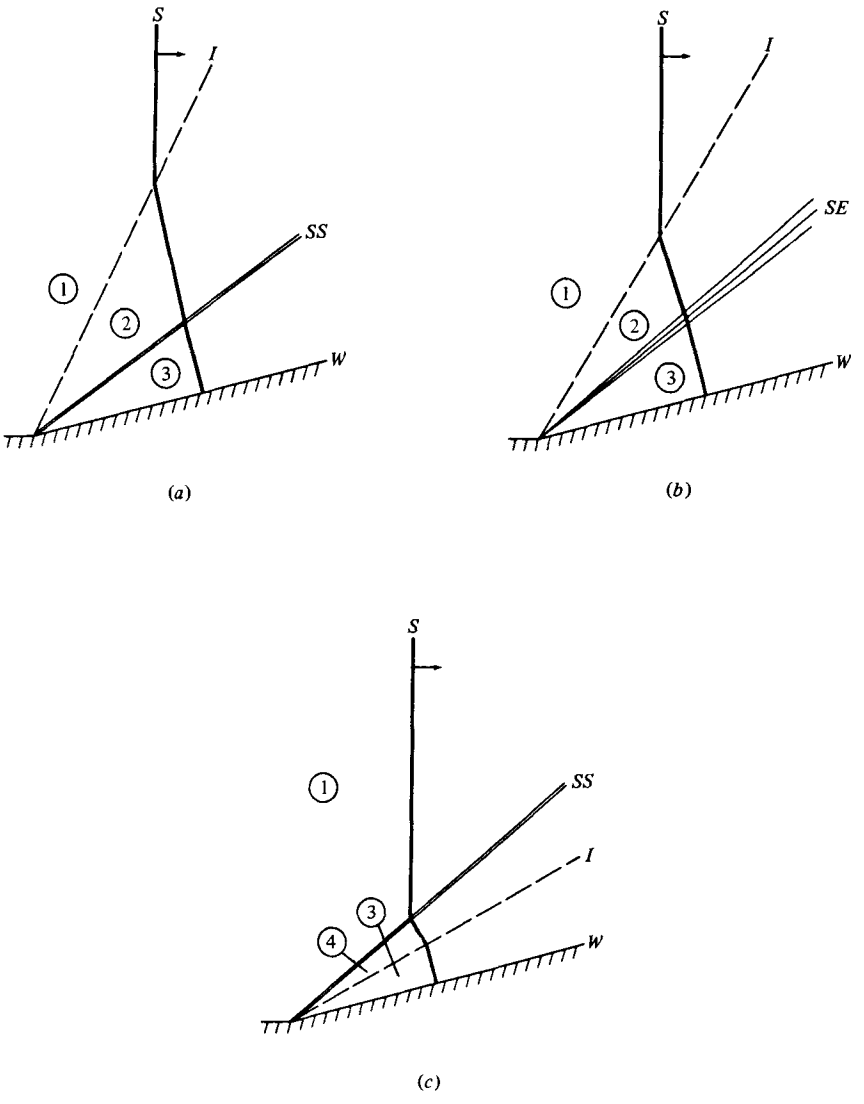

FIGURE 5. Solutions for problem 2 with $M_1 = 5{\cdot}0$, $a_{02}/a_{01} = 2{\cdot}0$ and $\delta_W = 15{\cdot}0°$: (*a*) regular refraction, $\delta_I = 65{\cdot}0°$ (case 16); (*b*) regular refraction, $\delta_I = 60{\cdot}0°$ (case 18); (*c*) irregular refraction, $\delta_I = 30{\cdot}0°$ (case 23); *S*, shock front; *I*, interface; *W*, wall; *SE*, shock–expansion; *SS*, shock–shock.

In the first and second sequences, we set $M_1 = 5{\cdot}0$ and $a_{02}/a_{01} = 2{\cdot}0$. For large interface angles and small wall slopes ($\delta_W < \theta_{3_t}$), a shock–shock lies *below* the interface, as shown in figure 5(*a*) (case 16). As the interface angle is decreased, the shock–shock weakens, degenerates to a C^+ characteristic (case 17), and is converted into a shock–expansion as shown in figure 5(*b*) (case 18). The transition from the shock–shock to the shock–expansion results in regions 2 and 3 becoming identical (case 17), and corresponds to a zero contribution from the corner signal, referred to by Jahn (1956). In figure 5(*a*) (case 16) the corner signal is a net compression, while in figure 5(*b*) (case 18) it is a net rarefaction.

$a_{02}/a_{01} = 2{\cdot}0$, $M_1 = 5{\cdot}0$ and $\delta_W = 15{\cdot}0°$

Case	δ_I	M_2	θ_2	M_3	θ_3	M_4	θ_4	χ
16	65·0°	3·65	13·1°	3·70	15·0°	—	—	37·5°
17	62·9°	3·68	15·0°	3·68	15·0°	—	—	(38·5°)
18	60·0°	3·73	18·3°	3·64	15·0°	—	—	—
19	55·7°	(4·07)	(32·2°)	3·57	15·0°	—	—	—
20	55·0°	—	—	3·53	15·0°	(8·71)	(52·3°)	55·0°
21	45·0°	—	—	3·25	15·0°	7·44	42·5°	48·0°
22	38·2°	—	—	3·15	15·0°	6·84	35·8°	43·7°
23	30·0°	—	—	3·05	15·0°	6·31	28·0°	38·9°

$a_{02}/a_{01} = 2{\cdot}0$, $M_1 = 5{\cdot}0$ and $\delta_W = 45{\cdot}0°$

Case	δ_I	M_2	θ_2	M_3	θ_3	M_4	θ_4	χ
24	60·0°	3·73	18·3°	4·64	45·0°	—	—	56·3°
25	57·8°	(3·81)	(22·0°)	4·58	45·0°	—	—	57·8°
26	57·3°	—	—	4·52	45·0°	(9·25)	(55·2°)	57·3°
27	50·0°	—	—	4·10	45·0°	8·22	49·1°	52·6°

$a_{02}/a_{01} = 2{\cdot}0$, $M_1 = 5{\cdot}0$ and $\delta_W = 60{\cdot}0°$

Case	δ_I	M_2	θ_2	M_3	θ_3	M_4	θ_4	χ
28	75·0°	3·58	6·8°	6·34	60·0°	—	—	62·4°
29	64·2°	(3·66)	(13·7°)	5·74	60·0°	—	—	64·2°
30	63·9°	—	—	5·67	60·0°	(11·36)	(63·1°)	63·9°
31	61·0°	—	—	5·36	60·0°	10·72	61·2°	62·2°

$a_{02}/a_{01} = 2{\cdot}0$, $\delta_I = 30{\cdot}0°$ and $\delta_W = 0°$

Case	M_1	M_2	θ_2	M_3	θ_3	M_4	θ_4	χ
32	5·0	—	—	2·75	0°	6·29	27·72°	38·7°
33	4·0	—	—	2·21	0°	5·05	28·14°	38·9°
34	3·0	—	—	1·67	0°	3·80	28·81°	39·0°
35	2·0	—	—	1·14	0°	2·53	29·79°	38·6°
36	1·8	—	—	1·05	0°	2·27	29·96°	38·3°
37	1·78	—	—	1·04	0°	2·24	29·98°	38·2°
38	1·77	—	—	1·04	0°	2·23	29·99°	38·2°

Values in parentheses denote vanishingly small regions.

TABLE 2. Summary of calculated refraction parameters for problem 2

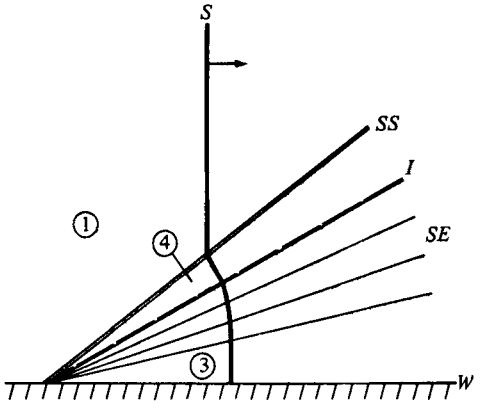

FIGURE 6. Irregular-refraction solution for problem 2 with $M_1 = 2{\cdot}0$, $a_{02}/a_{01} = 2{\cdot}0$, $\delta_W = 0°$ and $\delta_I = 30{\cdot}0°$ (case 35): S, shock front; I, interface; W, wall; SE, shock–expansion; SS, shock–shock.

As the interface angle is decreased further, the shock–expansion grows in size and strength until its upper C^+ characteristic lies adjacent to the interface (case 19). A further decrease in the interface angle results in the formation of a shock–shock just above the interface, that is, irregular refraction (case 20), and, as the interface angle becomes even smaller, the shock–shock separates from the interface (case 21), the shock–expansion vanishes (case 22) and, finally, a simple irregular refraction results, as shown in figure 5 (*c*) (case 23). In the limit, as the interface collapses onto the wedge ($\delta_I \rightarrow \delta_W$), the problem reduces to that of the irregular reflection of a shock by a wedge.

The second sequence of solutions occurs when the wall angle is large ($\delta_W > \theta_{3t}$). For large interface angles, as before, a shock–shock lies below the interface, between regions 2 and 3 (case 24). However, as the interface angle is decreased, the shock–shock moves towards the interface (case 25), crosses it (case 26), and moves out into the primary medium, resulting in a simple irregular-refraction result (case 27). The shock–shock is not converted into a shock–expansion, and the corner signal is compressive for all interface angles. In view of the fact that the order of crossing of the interface and the shock–shock by the C^- characteristics is reversed when the shock–shock passes through the interface (cases 25 and 26), it is remarkable that the conditions in region 3 nevertheless show the expected trend.

The larger the wall angle, the nearer the shock–shock remains to the wall for all interface angles (cases 28–31). Each of these solutions contains a tiny Mach stem, either at the wall (cases 28 and 29), or at the interface, when it is near the wall (cases 30 and 31). The Mach stem is the result of the boundary condition applied at the wall, and it is present even though the angles involved are large enough that the solutions should be regular. Thus, even in the limiting cases of $\delta_I = 90°$ and $\delta_I = \delta_W$, our solution predicts the presence of a tiny Mach stem at the wall, instead of giving a regular-refraction result.

In the third sequence we set $\delta_I = 30{\cdot}0°$ and $\delta_W = 0°$ (cases 32–38). As the incident shock strength is reduced, the strength of the shock at the wall M_3 tends to unity, and the shock front in region 4 becomes normal to the interface, as shown in figure 6 (case 35). It appears that both these limits are reached simultaneously, which is not surprising, since the conditions at the interface are influenced by the conditions at the wall. Physically, as the limit is approached, the shock–expansion behind the interface, which has been expanding downwards, fills the secondary medium entirely, and in the limit the ray tubes in region 4 do not cross the interface. If the incident shock strength were to be reduced or, alternatively, if the interface angle were to be decreased, the shock–expansion would have to expand further. This is not possible, and, since the expansion cannot be discontinuous, it appears that this situation is the limiting case for which the equations at the interface, (2.20) and (2.22), and the boundary conditions can be satisfied simultaneously. This can be interpreted to mean that, beyond this limit, the shock front should no longer be continuous across the interface. It has been observed experimentally that this situation leads to the formation of a precursor wave, that is, a discontinuous shock front at the interface, as discussed in §4.

The essential difference between the case of a normal shock at the interface for problem 1 (case 8), and the limiting case of a normal shock here, lies in the behaviour of the ray tubes. In problem 1 a portion of the shock front is present below the sloping part of the interface, having been transmitted through the vertical part, so that, as the interface angle passes through δ_{I_n}, the direction in which the ray tubes cross the interface is simply reversed. However, in the case of problem 2 the portion of the shock front below the interface comes *only* from the ray tubes that cross the interface

Regular refraction

Case	δ_I	M_1	a_{02}/a_{01}	Theoretical θ_3	Experimental θ_3
39	62°	1·073	1·289	9·0°	7°
40	47°	1·073	1·289	19·1°	19°
41	66°	1·073	0·780	−5·3°	−5°
42	27°	1·073	0·780	−19·3°	−19°
43	41°	1·732	0·780	−11·3°	−11°
44	32°	1·732	0·780	−15·8°	−15°

Irregular refraction – problem 2

Case	δ_I	δ_W	M_1	a_{02}/a_{01}	Theoretical M_3	Theoretical χ	Experimental M_3	Experimental χ
45	35°	25°	1·732	1·289	1·70	39·5°	1·69	37°
46	15°	1°	1·073	1·289	1·00	26·7°	1·00	21°

TABLE 3. Calculated and measured refraction parameters based on settings used by Jahn

from above. Thus, when the shock becomes normal to the interface, it appears that no further solution is possible by shock dynamics theory.

It is worth noting that, for the special case of the horizontal wall ($\delta_W = 0°$), by considering the wall to be an axis of symmetry one obtains the solution to the double-wedge problem, in which both faces of the gaseous wedge are inclined at equal angles to the undisturbed rays of the incident shock wave.

4. Comparison with experiment and theory

4.1. *Comparison with experimental results*

4.1.1. *Jahn's results.* Jahn (1956) published experimental results on shock refraction at a plane gaseous interface. He used gas combinations of air–methane and air/carbon dioxide, and the gases were prevented from mixing at the interface by a very thin plastic membrane. The results of computations based on the settings used in his experiments are presented in table 3, together with the experimental results that were measured from his published photographs. For the regular-refraction case, according to shock dynamics theory, the conditions in region 3 are determined solely from the conditions in region 1, so that the comparison with experiment is only local. For the irregular-refraction case, however, the conditions at the interface are influenced by the presence of the wall, so that it is necessary to consider the whole flow field.

In order to locate the shock–shock in the photographs, the position of the corner had to be determined by extending the lines along the interface and the wall upstream until they intersected. Since the angle between the interface and the wall is small in both cases 45 and 46, this introduces a possible error in the measured value for χ. Further, in all four cases the ratio γ_2/γ_1 is approximately 0·93, whereas in the computations γ_2/γ_1 has been taken to be unity. Nevertheless, it is seen from the table that the calculated values compare favourably with the values measured from the photographs.

Case 46, which is based on figure 14(*e*) of Jahn's paper, requires special comment. The experimental result has a discontinuous main shock front and a precursor wave at the interface. Shock dynamics, however, attempts to find a solution in which the main shock front is continuous across the interface. The solution for this case does not converge to within the specified tolerance, and the computational accuracy is only

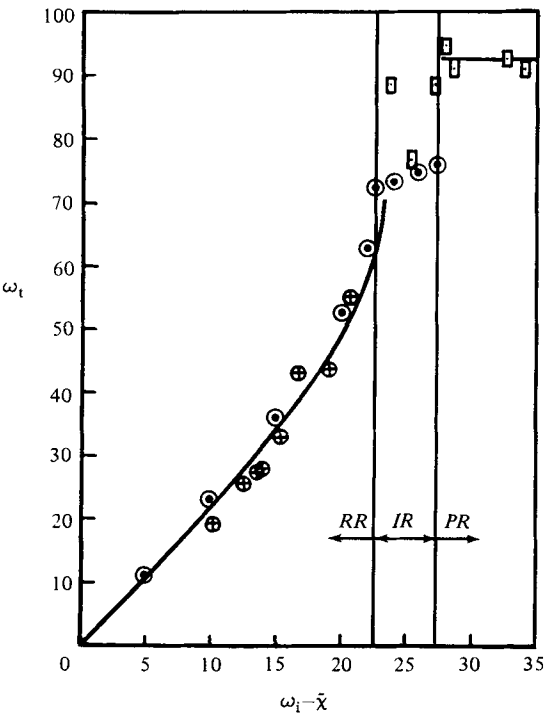

FIGURE 7. Transmitted shock wave angle ω_t versus incident shock wave angle ω_i for refraction of a plane shock at a contaminated carbon dioxide/helium interface: ⊙, present theory; ⊕, experimental results (regular refraction); ⊡, experimental results (irregular refraction); —, best-fit curves of Abd-el-Fattah *et al.* for the experimental data; *RR*, regular refraction; *IR*, irregular refraction; *PR*, precursor irregular refraction.

1 %, indicating that the equations and the boundary conditions cannot be satisfied simultaneously. This is consistent with the experimental result that, under these conditions, the shock front is not continuous at the interface.

4.1.2. *Abd-el-Fattah, Henderson & Lozzi's results.* Abd-el-Fattah *et al.* (1976) have performed a series of experiments on shock refraction using a set-up similar to that of Jahn. In order to obtain as large a sound-speed ratio as possible, they used a carbon dioxide/helium gas combination across the interface. They observed that the gases leaked through the membrane, and, using a gas analyser, they record that, at the time the shock tube was fired, the carbon dioxide was about 95 % pure (5 % by volume helium) and the helium was about 90 % pure (10 % by volume carbon dioxide).

Shown in figure 7, which is reproduced from Abd-el-Fattah *et al.*, is the observed transmitted shock wave angle ω_t versus the incident shock wave angle ω_i. The wave angles ω_i and ω_t are related to our notation

$$\omega_i = 90° - \delta_I, \tag{4.1}$$

$$\omega_t = \theta_t + (90° - \delta_I), \tag{4.2}$$

$$\tilde{\chi} = \chi - \delta_I, \tag{4.3}$$

where θ_t is the ray angle of the transmitted shock front at the interface.

The results of our calculations have been entered in the figure. These calculations are based on a contaminated carbon dioxide/helium interface, across which $a_{02}/a_{01} = 2{\cdot}53$, but we have taken the ratio γ_2/γ_1 across the interface to be unity,

instead of using the actual value of 1·22. Further, it has been assumed that the back plate is in line with the front plate, that is, $\delta_W = 0°$. Agreement with the experimental results is very good, and over the whole range of incident wave angles, from $\omega_i = 0°$ through transition, the present theory provides a much better model than either the Snell–piston theory or the piston–diaphragm theory of Abd-el-Fattah *et al.* (1976). We find that transition from regular to irregular refraction occurs at $\omega_i = 22·7°$, which compares with $\omega_i = 23·12°$ at transition from the three-shock theory, discussed in §4.2.

Over the range $22·7° < \omega_i < 27·6°$, the refraction is irregular and a shock–shock lies above the interface. (Between $\omega_i = 22·7°$ and $\omega_i = 24·0°$, no solution could be obtained, for reasons that are given in §3.1). The angle $\tilde{\chi}$ between the shock–shock and the interface is small, reaching a maximum value of 0·25° at $\omega_i = 27·6°$, which would explain why the shock–shock and the Mach stem are hardly discernible from the interface in figure 13 (plate 3) of Abd-el-Fattah *et al.* Further, the transmitted shock wave angle *at the interface* changes from $\omega_t = 73·6°$ at $\omega_i = 24·0°$ (transition), to $\omega_t = 76·4°$ at $\omega_i = 27·6°$, and does not approach the experimentally observed value of $\omega_t = 93·0°$ for large incident wave angles. The reason for this discrepancy is that the solution according to shock dynamics theory is constrained to predict a shock front that is continuous throughout, whereas the experiments show a discontinuous shock front at the interface.

This range of incident wave angles corresponds to the bound-precursor range discussed by Abd-el-Fattah *et al.* Their photographs show that, in this range, the transmitted wave is slightly ahead of the incident wave at the interface. Although their results were not conclusive, they noticed, however, that both the incident and transmitted shock fronts had the same, or very nearly the same, velocity along the interface, and they inferred that the discontinuity of the shock front at the interface is the result of some non-pseudostationary process at the corner. Perhaps, if the secondary effects of the corner could be eliminated completely (i.e. if the back plate were to be aligned perfectly with the front plate with no gap between them) then the bound-precursor irregular-refraction result would indeed reduce to a simple irregular-refraction result.

For $\omega_i > 27·6°$, shock dynamics theory does not yield any solution. As discussed in §3.2, this is because, as the incident wave angle approaches the limit of $\omega_i = 27·6°$, the shock–expansion behind the interface fills the entire region, and, at the same time, the shock front at the interface becomes normal to the interface, so that no ray tubes cross the interface. This range of incident wave angles corresponds to the free-precursor result discussed by Abd-el-Fattah *et al.* in which the velocity V_t of the precursor (transmitted wave) is greater than the velocity V_i of the incident shock along the interface. In their paper they determine the incident wave angle for the second transition, that is, the transition to the free-precursor result, to be $\omega_i = 28·8°$ or 27·4°, depending on whether or not the membrane inertia is considered. These values compare very favourably with our result of 27·6°.

4.1.3. *Abd-el-Fattah & Henderson's results.* In a subsequent paper, Abd-el-Fattah & Henderson (1978) studied shock-wave interactions at a carbon dioxide/methane interface. They used three different incident shock strengths, namely $M_1 = 1·118$, 1·336 and 2·243, which they classified as the very weak group, the weak group and the strong group respectively. In general, for each of the three groups, at small wave angles, the refraction was regular. This was followed by bound-precursor irregular refraction for larger wave angles and by various types of free-precursor irregular refractions at very large wave angles. These results are qualitatively the same as those

discussed in §4.1.2, except for the occurrence of the different kinds of irregular refraction in the free-precursor range.

For the very weak group, the agreement between Abd-el-Fattah & Henderson's experimental results and our shock dynamics computations is very good, especially for the regular-refraction range, and the limits of their bound-precursor range correspond almost exactly to the limits of our irregular-refraction range. However, for the weak group and the strong group, good agreement is obtained only in the regular-refraction range. For the weak group, we find that the irregular-refraction range extends from transition at an interface angle of 53·2° to an interface angle of 29°, whereas Abd-el-Fattah & Henderson indicate that the bound-precursor range extends from transition at an interface angle of about 53° to an interface angle of about 44° only. For the strong group, shock dynamics predicts irregular refraction from transition at $\delta_I = 51{\cdot}6°$ through to $\delta_I = 0°$, that is, until the interface lies on the wall. On the other hand, Abd-el-Fattah & Henderson give a bound-precursor result in the range $49{\cdot}7° > \delta_I > 33{\cdot}4°$, and for interface angles smaller than 33·4° their observations indicate a free-precursor result.

Despite the poor agreement between the limits for the ranges of Abd-el-Fattah & Henderson's bound-precursor refraction results and our irregular-refraction results, it is interesting to note that their trajectory path angles of the shock-wave confluences, χ_1 and χ_2, show satisfactory agreement with our shock–shock angle. This appears to indicate that the general forms of the shock refraction in both the experiment and the theory are the same, and suggests that the various bound-precursor results observed may have been caused by the experimental set-up.

The reason for these discrepancies is not clear at this time. As Abd-el-Fattah & Henderson have pointed out, their results do not agree entirely with the results obtained by Jahn (1956), and in particular they do not record any cases of irregular refraction in which the transmitted wave is continuous with the Mach stem, as shown in Jahn's figure 14(*c*). Their experimental results also indicate that for large wave angles, that is, for small interface angles, a corner signal attenuates the reflected wave at the three-shock confluence. As mentioned in §4.1.2, this corner signal may be a result of the experimental set-up. It appears that further analysis will be required when more experimental data becomes available.

4.2. *Comparison with three-shock theory*

Abd-el-Fattah *et al.* (1976) have computed the transition angles for refraction of a plane shock at a pure carbon dioxide/helium interface as a function of the incident shock strength. They use a method developed by Henderson (1966), based on the behaviour of three shock waves meeting at a point, in which the full equations of motion are applied to the *local* shock geometry at the interaction point on the interface, and are solved graphically in the hodograph plane using the shock polar method. Their results are shown by the solid line in figure 8, which is reproduced from their paper, where the variable η_i is

$$\eta_i = \frac{2\gamma M_1^2 - (\gamma - 1)}{\gamma + 1}. \tag{4.4}$$

The results of the present theory have been entered as data points in the figure. It is seen that, for Mach numbers below 3, the agreement is very good. Again, for simplicity, we have taken the ratio γ_2/γ_1 across the interface to be unity, instead of using the actual value of 1·28.

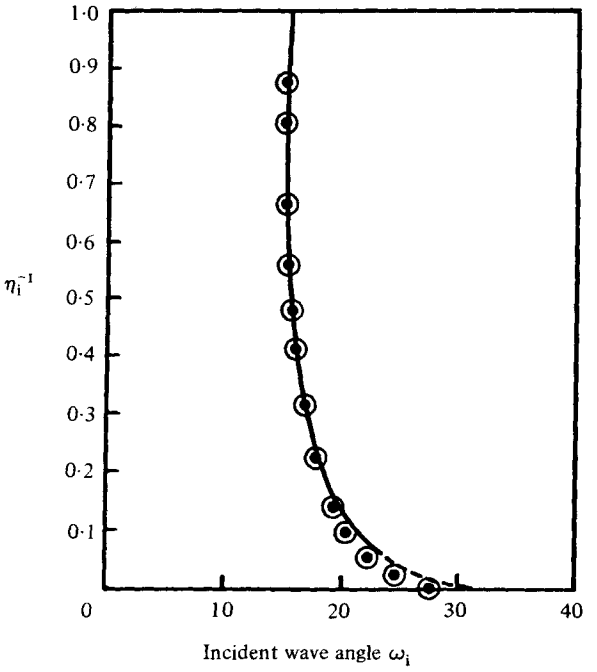

FIGURE 8. Transition angles for refraction of a plane shock at a pure carbon dioxide/helium interface: ⊙, present theory; —, results of Abd-el-Fattah *et al.*

Case	M_1	a_{02}/a_{01}	M_2	θ_2	M_3	θ_3
47	1·5	1·5	1·39	0°	1·40	0°
48	1·5	5·0	1·15	0°	1·20	0°
49	5·0	1·5	4·03	0°	4·08	0°
50	5·0	5·0	2·09	0°	2·42	0°

TABLE 4. Calculated refraction parameters for normal interaction

4.3. *Normal interaction*

An interesting check of the accuracy of the theory can be made in the case of problem 1 with $\delta_I = 90°$, for which the shock interacts normally with the interface (table 4). Since the transmitted wave in region 2 is calculated exactly in this analysis from the one-dimensional gasdynamics equations, while the transmitted wave in region 3 is calculated approximately by shock dynamics theory, the departure of M_3 from M_2 and of θ_3 from 0 provide a measure of the accuracy of the theory. It is seen that the theory shows reasonable agreement, although the accuracy decreases as the ratio a_{02}/a_{01} increases, as might have been expected. The results of a more complete analysis of this case are depicted in figure 9, in which the error ϵ is defined by $\epsilon = (M_3 - M_2)/M_2$.

5. Summary and conclusions

In this paper, Whitham's theory of shock dynamics has been reformulated to account for imposed non-uniformities in the undisturbed medium ahead of the shock

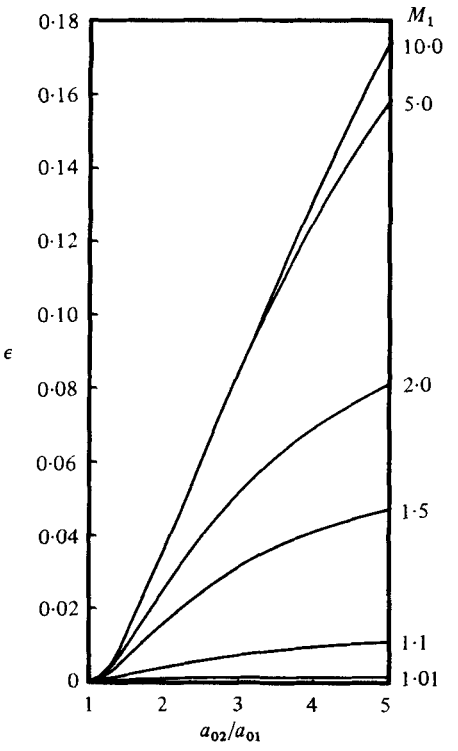

FIGURE 9. Relative error between the results from shock dynamics and the results from one-dimensional gasdynamics for normal interaction, $\delta_I = 90°$.

front. The governing equations are hyperbolic in nature. When compared with the conventional shock dynamics equations for a uniform medium, the essential difference is the appearance of source terms, which represent disturbances generated on the shock front as the shock propagates into regions where the fluid properties are non-uniform.

As in the case of a uniform medium, discontinuities of shock strength M and slope θ can occur in the form of shock–shocks, which are the manifestation of the triple-shock intersections in Mach reflection. However, the presence of a contact surface, across which there exists an imposed change in fluid properties, introduces another kind of discontinuity in the shock front. Jump conditions across the interface are developed from the characteristic equations, and the theory *naturally* provides a relationship analogous to Snell's law. The shock dynamics equations governing shock refraction at a gaseous interface are simple to apply and yield a unique solution. By changing various parameters such as the incident shock strength, the fluid property ratios across the interface, and the interface angle, a large variety of interesting configurations are easily obtained. These features give the present theory its greatest appeal over existing methods for calculating shock refraction.

The theory models both regular refraction and irregular refraction, and also predicts the transition from one to the other. This is in contrast with the diffraction of shock waves in a uniform medium over solid wedges, where the theory only models irregular refraction. Transition from regular to irregular refraction in shock dynamics theory is analogous to the transition which occurs in unsteady one-dimensional

gasdynamics under the action of a moving force field or 'leaky piston', in which the solution changes from one that is shock-free for a supersonic force to one that contains a shock for a subsonic force. In both problems, a sonic configuration occurs that is analogous to Chapman–Jouget detonation.

For irregular refraction, given an incident shock strength and fluid property ratio, there exists an interface angle at which the Mach stem is normal to the interface, so that no rays cross the interface. This is the condition for no energy flow across the interface, and it is the same condition that is applied at a solid boundary in the analysis of shock diffraction using the theory of shock dynamics in a uniform medium.

In the neighbourhood of a solid boundary, under certain conditions, a limiting irregular case is obtained, in which the Mach stem becomes normal to the interface, and the Mach number of the shock front at the wall tends to unity. It appears that this signals the onset of a discontinuous shock front at the interface, namely the formation of a precursor wave.

It has been implicitly assumed, through the application of the characteristic rule, that modifying disturbances overtaking the main shock front are excluded. Further, as pointed out by Whitham (1957), the theory tends to overconcentrate the disturbances on the shock front. For strong shocks this representation is satisfactory, but for weak shocks the true disturbance is distributed over a larger region than predicted by the theory. In spite of these factors, it appears that the calculated shock parameters compare favourably with the limited experimental data available. In particular, the calculated wave angles for the transmitted shock in regular refraction show very good agreement with experiment, while the calculated angles for transition from regular to irregular refraction agree well with the predictions from three-shock theory.

Future work will be directed at investigating problems involving the fast–slow gaseous interface, and also at examining shock refraction problems in which the variation of fluid properties is continuous.

The authors are grateful to Professor G. B. Whitham for drawing their attention to the analogy between a contact discontinuity in shock dynamics and a moving force in unsteady gasdynamics. This work was supported by the National Science Foundation under Grant CME-7822089.

REFERENCES

Abd-el-Fattah, A. M. & Henderson, L. F. 1978 Shock waves at a slow–fast gas interface. *J. Fluid Mech.* **89**, 79–95.

Abd-el-Fattah, A. M., Henderson, L. F. & Lozzi, A. 1976 Precursor shock waves at a slow–fast gas interface. *J. Fluid Mech.* **76**, 157–176.

Chester, W. 1954 The quasi-cylindrical shock tube. *Phil. Mag.* **45** (7), 1293–1301.

Chisnell, R. F. 1955 The normal motion of a shock wave through a non-uniform one-dimensional medium. *Proc. R. Soc. Lond.* **A232**, 350–370.

Chisnell, R. F. 1957 The motion of a shock wave in a channel, with applications to cylindrical and spherical shock waves. *J. Fluid Mech.* **2**, 286–298.

Collins, R. & Chen, H. T. 1970 Propagation of a shock wave of arbitrary strength in two half planes containing a free surface. *J. Comp. Phys.* **5**, 415–422.

Collins, R. & Chen, H. T. 1971 Motion of a shock wave through a non-uniform fluid. In *Proc. 2nd Int. Conf. on Numerical Methods in Fluid Dynamics* (ed. M. Holt). Lecture Notes in Physics, vol. 8, pp. 264–269. Springer.

HENDERSON, L. F. 1966 The refraction of a plane shock wave at a gas interface. *J. Fluid Mech.* **26**, 607–637.

HOFFMAN, A. L. 1967 A single-fluid model for shock formation in MHD shock tubes. *J. Plasma Phys.* **1**, 193–207.

HORNUNG, H. G., OERTEL, H. & SANDEMAN, R. J. 1979 Transition to Mach reflection of shock waves in steady and pseudosteady flow with and without relaxation. *J. Fluid Mech.* **90**, 541–560.

JAHN, R. G. 1956 The refraction of shock waves at a gaseous interface. *J. Fluid Mech.* **1**, 457–489.

KUTLER, P. & SHANKAR, V. 1977 Diffraction of a shock wave by a compression corner: part II – single Mach reflection. *A.I.A.A. J.* **15**, 197–203.

POLACHEK, H. & SEEGER, R. J. 1951 On shock-wave phenomena; refraction of shock waves at a gaseous interface. *Phys. Rev.* **84**, 922–929.

SHANKAR, V., KUTLER, P. & ANDERSON, D. 1978 Diffraction of a shock wave by a compression corner: part I – regular refraction. *A.I.A.A. J.* **16**, 4–5.

TAUB, A. H. 1947 Refraction of plane shock waves. *Phys. Rev.* **72**, 51–60.

WHITHAM, G. B. 1957 A new approach to problems of shock dynamics. Part 1. Two-dimensional problems. *J. Fluid Mech.* **2**, 145–171.

WHITHAM, G. B. 1958 On the propagation of shock waves through regions of non-uniform area or flow. *J. Fluid Mech.* **4**, 337–360.

WHITHAM, G. B. 1959 A new approach to problems of shock dynamics. Part 2. Three-dimensional problems. *J. Fluid Mech.* **5**, 369–386.